

Spin-polaron excitations in a doped Shastry-Sutherland model

S. El Shawish¹ and J. Bonča²¹*J. Stefan Institute, SI-1000 Ljubljana, Slovenia*²*Faculty of Mathematics and Physics, University of Ljubljana, SI-1000 Ljubljana, Slovenia*

(Received 2 August 2006; revised manuscript received 25 September 2006; published 17 November 2006)

Using variational algorithm on an infinite Shastry-Sutherland (SS) lattice we show that the introduction of a static nonmagnetic impurity into a dimerized ground state leads to a formation of a small, localized spin polaron surrounding the impurity site. Due to a particular symmetry of the SS lattice, the polaron is extremely anisotropic with a short spatial extent. The presence of nonmagnetic impurities leads to a formation of pronounced in-gap peaks in the dynamical spin structure factor, which we attribute to the spin-doublet excitations of a single unpaired spin $S=1/2$ surrounded by triplet fluctuations. Our results are relevant for the description of $\text{SrCu}_2(\text{BO}_3)_2$ compound when doped with nonmagnetic atoms at Cu sites.

DOI: [10.1103/PhysRevB.74.174420](https://doi.org/10.1103/PhysRevB.74.174420)

PACS number(s): 75.10.Jm, 75.30.Hx, 75.40.Gb, 75.50.Mm

I. INTRODUCTION

The relation between disordered spin liquids with a gap in the spin excitation spectrum and superconductivity has aroused a lot of interest. It was suggested¹ that doping a gapped system may lead to hole pairing and superconductivity. In this sense the idea of finding a superconducting state in a doped two-dimensional spin-liquid $\text{SrCu}_2(\text{BO}_3)_2$ compound, representing the first physical realization of the Shastry-Sutherland (SS) model,^{2–4} has been proposed^{5–7} due to its structural similarity with the high-temperature cuprates. So far, numerical calculations do not seem to support superconductivity in the doped SS model.⁸

Another aspect of the study of the doped $\text{SrCu}_2(\text{BO}_3)_2$ is the influence of impurities on the nature of the singlet (dimerized) ground state. When J'/J of the underlying SS model is close to but below the critical value ~ 0.7 ,⁴ at finite doping, the system may select other ordered or disordered states, which may in turn strongly affect the magnetism of this material. It is rather straightforward to realize that replacing magnetic Cu ions with nonmagnetic ones breaks the singlet nature of the bonds, thus providing an additional frustration, resulting in the reduction of the spin gap. The effects of doping should materialize in inelastic neutron scattering through enhanced lifetimes of single-triplet excitations—magnons. A finite lifetime associated with magnon scattering on spin excitations surrounding the nonmagnetic ions would in turn lead to a broadening of the single-triplet peak line in the doped $\text{SrCu}_2(\text{BO}_3)_2$.

The SS model consists of a relatively simple spin ($S=1/2$) Hamiltonian,

$$H = J \sum_{\langle i,j \rangle} \mathbf{S}_i \cdot \mathbf{S}_j + J' \sum_{\langle i,j \rangle'} \mathbf{S}_i \cdot \mathbf{S}_j, \quad (1)$$

here $\langle i,j \rangle$ denotes the nearest neighbors (NN) on bonds J (dimers) and $\langle i,j \rangle'$ next-nearest neighbors (NNN) on bonds J' . We introduce a single nonmagnetic impurity—a site with a missing spin, into the model in Eq. (1). It is well known that for $J'/J \leq 0.7$ the exact ground state can be written as a product of singlet dimers.⁴ We should stress that the introduction of a single hole into the exact dimerized ground state has nontrivial consequences.

Previous theoretical studies have been focused mostly on the doping of SS model with mobile holes,^{5,7–9} with the intention to explore the hole-pairing mechanism relevant for superconductivity. In our work we limit our investigations to one static nonmagnetic impurity (magnetic polaron) within the SS lattice. Our calculations are relevant to the case where the substitution with nonmagnetic ions takes place at Cu sites. We use a variational method within a variational space constructed by successively applying the off-diagonal parts of Hamiltonian (1) on the starting (0th-generation) state vector. The method yields converged results, valid within the infinite system, for static quantities such as the value of the spin gap as well as for the spin distribution function. We also explore the properties of the first few low-lying excited spin-polaron states. Finally, we compute the dynamical spin structure factor as a function of the wave vector.

For simplicity, we have decided to neglect the anisotropic Dzyaloshinsky-Moriya interactions originating in spin-orbit coupling¹⁰ and used the (bare) SS Hamiltonian (1).

II. VARIATIONAL APPROACH IN 1-HOLE LIMIT

A variational space was constructed by starting from the 0th-generation state vector $|1_0\rangle$ representing one doped hole with a neighboring uncoupled spin within a sea of singlet dimers [Fig. 1(a)]. First generation, $M=1$, of variational states was consequently obtained by acting with H (1) on state $|1_0\rangle$. Successive generations leading to M th order states $\{|i_M\rangle\}$ were obtained starting from all previously generated ones $\{|i_{M-1}\rangle\}$. A state can be uniquely determined by the orientation of the spin adjacent to the impurity site, $S_u^z = \pm 1/2$, and the arrangement of $S^z=0, +1$ and -1 triplet dimers in the vicinity of the hole, $\{\mathbf{r}_i^0\}$, $\{\mathbf{r}_i^{+1}\}$, and $\{\mathbf{r}_i^{-1}\}$, respectively. With $\mathbf{r}_i^{S^z}$ we denote the positions of triplet-dimer centers relative to the impurity site. i th variational state within M th generation is thus written as

$$|i_M\rangle \equiv |S_u^z, \{\mathbf{r}_i^0\}, \{\mathbf{r}_i^{+1}\}, \{\mathbf{r}_i^{-1}\}\rangle, \quad (2)$$

where a fixed ordering of $\mathbf{r}_i^{S^z}$ vectors is assumed to prevent double counting. In this notation the initial state is written as $|1_0\rangle = |1/2, \{\}, \{\}, \{\}\rangle$. In a similar fashion we can also describe the (exact) 0-hole ground state.

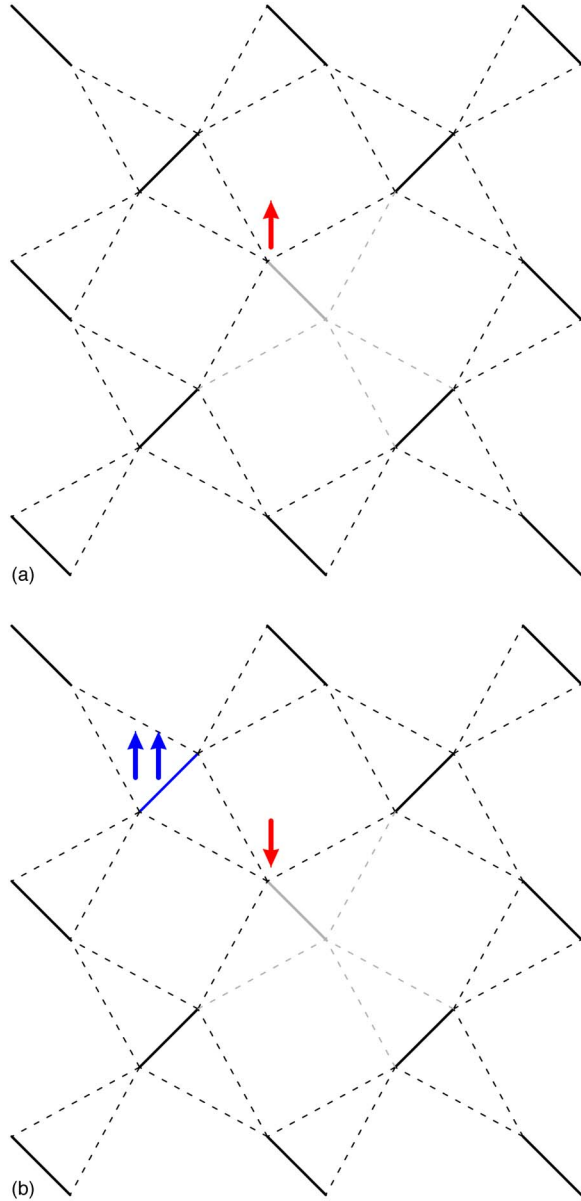


FIG. 1. (Color online) Two initial states ($M=0$) in the 1-hole variational procedure defined on infinite SS lattice: (a) state $|1_0\rangle$ with uncoupled spin $S_u^z=1/2(\uparrow)$ within a sea of singlet dimers (black solid lines), and (b) state $|2_0\rangle$ with $S_u^z=-1/2(\downarrow)$ and one $S^z=1$ triplet dimer ($\uparrow\uparrow$). Dashed black lines denote off-diagonal terms (J') of H (1).

An advantage of the introduced procedure, in which a variational space grows like $N_{\text{st}} \sim 6^M$ (see Table I), is that triplet dimers of newly generated variational states develop gradually around a hole, which is very promising in a way that only a few such states would suffice to correctly describe the localized nature of the spin polaron found in Refs. 8 and 9. As application of the off-diagonal part (J') of Hamiltonian H on inter-singlet-dimer bonds is zero, the relevant region from where new triplets may be generated is limited to a neighborhood of the hole. Due to specific topology of the SS lattice, a gradual expansion of triplet region with increasing M is proceeded in a zig-zag path. A short calculation shows that already $M=3$ is enough for the outermost triplet to ex-

TABLE I. Variational calculation for $J=76.8$ K, $J'/J=0.62$. M (N_{st}) denotes the number of variational steps (states) and $\Delta^{(0)} = E_1^{(0)}(S=1) - E_0^{(0)}(S=0)$ represents the spin gap of the undoped system. $E_0^{(1)}$ is the ground state energy of the 1-hole system measured relative to the ground state energy $E_0^{(0)}(S=0)$ of the 0-hole system. $\Delta^{(1)} = E_1^{(1)}(S=1/2) - E_0^{(1)}(S=1/2)$ and $\Lambda^{(1)} = E_2^{(1)}(S=1/2) - E_0^{(1)}(S=1/2)$ where $E_1^{(1)}(S=1/2)$ and $E_2^{(1)}(S=1/2)$ represent the first and second excited states of the 1-hole system, respectively. We also show extrapolated values for $M \rightarrow \infty$. All energies are listed in meV.

M	0-hole system		1-hole system			
	N_{st}	$\Delta^{(0)}$	N_{st}	$E_0^{(1)}$	$\Delta^{(1)}$	$\Lambda^{(1)}$
0	3		2			
1	11	4.206	13	3.852	2.486	5.679
2	59	3.507	78	3.525	1.976	3.423
3	377	3.225	507	3.416	1.784	2.525
4	2469	3.100	3354	3.379	1.690	2.100
5	16186	3.042	22141	3.368	1.634	1.903
6	105663	3.015	145402	3.364	1.604	1.820
7	686111	2.998	948025	3.363	1.584	1.777
8	4429695	2.983	6144089	3.363	1.576	1.762
∞		2.979		3.362	1.573	1.745

ceed the square region of 32 sites used in Ref. 8.

Along with the construction of the variational space we calculated nonzero matrix elements $H_{ij}^M = \langle i_M | H | j_{M-1} \rangle$ separately for each term in Hamiltonian (1). In this way, a matrix representation of H was written in a block-diagonal form with k th ($k=1, \dots, M$) block corresponding to submatrix $[H_{ij}^k]$. A whole matrix H was then diagonalized at each generation M to control the convergence. We used a standard exact-diagonalization technique for $M \leq 5$ and an efficient Lanczos approximation for a few lowest eigenenergies when $M \geq 5$. In Fig. 2 we show the convergence of a few lowest eigenenergies for the 1-hole and, for comparison, also for the 0-hole case. Concentrating first on the single impurity case, we plot the energy difference between the ground state and the first two excitations, $\Delta^{(1)}$ and $\Lambda^{(1)}$, as a function of J'/J at fixed $J=76.8$ K. In this particular calculation two initial state vectors were used to improve the sampling of the variational space: $|1_0\rangle$ and $|2_0\rangle = |-1/2, \{\}, \{(0,1)\}, \{\}$ with one $S^z=1$ triplet located above the uncoupled spin as also depicted in Fig. 1(b). This choice seems to be optimal for obtaining good convergence of the ground state as well as of the first excited state. In addition, we choose to work in the $S^z=1/2$ sector that contains the ground state of the 1-hole system in the absence of the magnetic field. No other symmetries were explicitly employed in the construction of the variational space. The SS model doped with a static hole possesses the mirror symmetry over the plane containing a doped dimer. We have checked that eigenstates and corresponding correlation functions transform according to this symmetry.^{11,12}

Moving back to the convergence of results for the 1-hole case, as presented in Fig. 2, we notice, that values of $\Delta^{(1)}$ and $\Lambda^{(1)}$ have nearly converged for $J'/J \leq 0.62$ for $M=8$, i.e.,

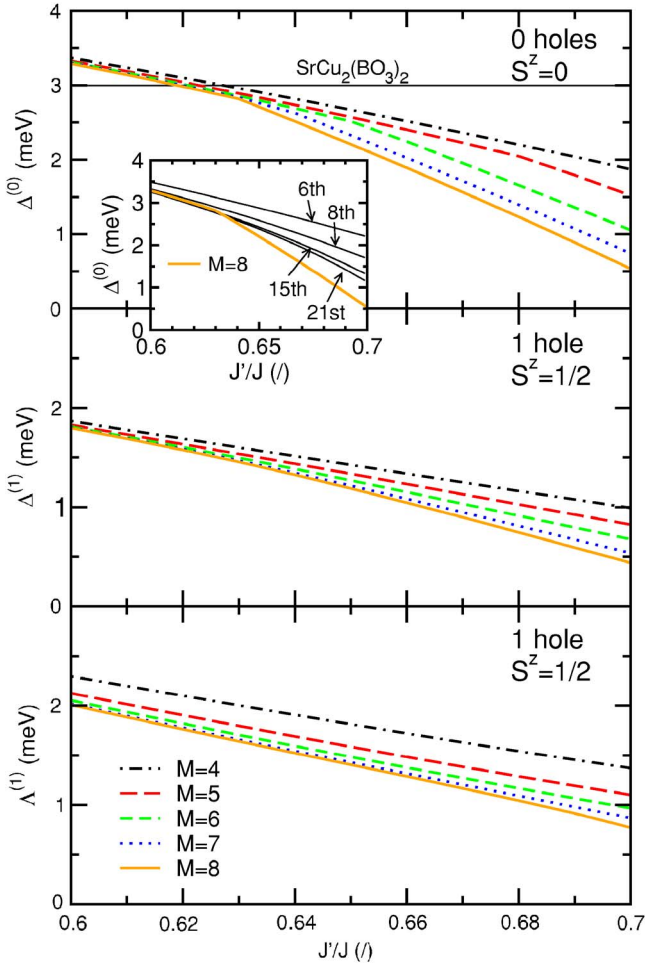


FIG. 2. (Color online) Energies relative to the ground-state energy vs J'/J calculated at $J=76.8$ K for 0- and 1-hole system, defined on infinite SS lattice, using M steps of the variational method. Black solid line represents experimental value obtained on $\text{SrCu}_2(\text{BO}_3)_2$. In the inset we show the comparison with the 6th, 8th, 15th, and 21st order dimer-expansion calculation in J'/J for 0 holes (Refs. 16 and 17).

their values at $M=8$ are not far from their extrapolated values for $M \rightarrow \infty$. As expected, the variational approach becomes worse when J'/J approaches the transition to the AFM state of the 0-hole case, $J'/J \sim 0.7$. This can be better seen in a 0-hole case where the spin gap $\Delta^{(0)}$ should close as $J'/J \rightarrow 0.7$. In our calculations $J'/J \sim 0.64$ represents a critical ratio beyond which the convergence of the spin gap $\Delta^{(0)}$ is lost. On the other hand, at $J'/J=0.62$ a single-triplet energy is quite well converged for $M=8$, which in turn leads to thermodynamically converged value of the spin gap $\Delta^{(0)}$ that also agrees with the experimental value $\Delta^{(0)} \sim 3$ meV. This suggests that the same set of J and J' as in calculations on 20 sites^{13–15} may be used here in order to compare with realistic $\text{SrCu}_2(\text{BO}_3)_2$ system. We attribute this fast convergence to the thermodynamic limit to the fact that single-triplet excitations are well localized, which renders a limited variational space sufficient for nearly exact description of low-energy excitations.

A 0-hole case may also serve as a test for the method, for it can be directly compared to alternative approximate ap-

proaches. A comparison with dimer-expansion technique of Zheng *et al.*¹⁶ and Knetter *et al.*¹⁷ is shown in the inset of Fig. 2. Our method for $M=8$ gives similar energy-gap dependence as the 21st order calculation for $J'/J \leq 0.64$, however, at larger values of $J'/J \geq 0.64$ our method captures better the closing of the spin gap. It should be noted at this point that even better convergence with M is expected when a translational symmetry of the lattice is employed for the 0-hole case.

Given the finite size of the variational space (N_{st}), the results of the introduced method depend on the choice of the initial states $\{|i_{M=0}\rangle\} = \{|1_0\rangle, |2_0\rangle, \dots\}$. By definition, the optimally chosen $\{|i_0\rangle\}$ provides the lowest energy of a particular eigenstate of interest, for example, the ground state. As we show later, in the ground state a spin polaron is centered around the impurity site, therefore $\{|i_0\rangle\}$ with triplets in this region would be good initial states (see Fig. 1). There is, however, no point in searching for optimal $\{|i_0\rangle\}$; we have checked numerically that an error introduced by taking a reasonably good but not optimal $\{|i_0\rangle\}$ is always lower than an energy drop when the next variational step is taken. In this respect, we used a simple rule of thumb in our calculations by taking a few initial states with largest weights in the final ground state.

III. RESULTS

We have calculated the shape of a single spin polaron, forming in the vicinity of a static hole, as measured by the spin distribution function calculated in the 1-hole (by hole we denote the magnetic impurity) eigenstate $|n^{(1)}\rangle$ of H (1),

$$S_n^z(\mathbf{r}) = \langle n^{(1)} | S_{\mathbf{r}}^z | n^{(1)} \rangle, \quad n = 0, 1, 2. \quad (3)$$

Here \mathbf{r} denotes the position of the spin with respect to the hole. We first note that in the case of $J'/J \leq 0.7$ and zero doping $S_n^z(\mathbf{r})=0$ for all \mathbf{r} due to a singlet nature of the ground state $|0^{(0)}\rangle$.

In Fig. 3 we present the shape of the spin polaron, $S_0^z(\mathbf{r})$, and of its two lowest excitations, $S_1^z(\mathbf{r})$ and $S_2^z(\mathbf{r})$, calculated for $M=8$. The zero value of $S_n^z(\mathbf{r})$ indicates that \mathbf{r} points either towards the edges of a singlet or a $S^z=0$ triplet dimer. Note also that the following sumrule holds: $\sum_{\mathbf{r}} S_n^z(\mathbf{r}) = 1/2$. From Fig. 3 it is apparent that the ground state of the spin polaron is rather well localized around the impurity. Only the first two neighbors lying in the direction perpendicular to the dimer containing the impurity are strongly affected by the presence of the impurity. The other two neighbors lying along the direction of the dimer with the impurity are nearly unaffected giving $S_0^z(\mathbf{r}) \approx 0$. The shape of the spin polaron is therefore extremely anisotropic. This is in agreement with the exact $T=0$ calculations on 32 sites.⁸ According to Ref. 8, a mobile hole introduced to the dimerized ground state forces the resulting free spin to minimize the energy by forming a five-spin chain with two of its nearest dimers. This excitation is localized and has a small dispersion compared to the t - J model on a square lattice. These results are in qualitative agreement with our small-spin-polaron picture around the localized hole.

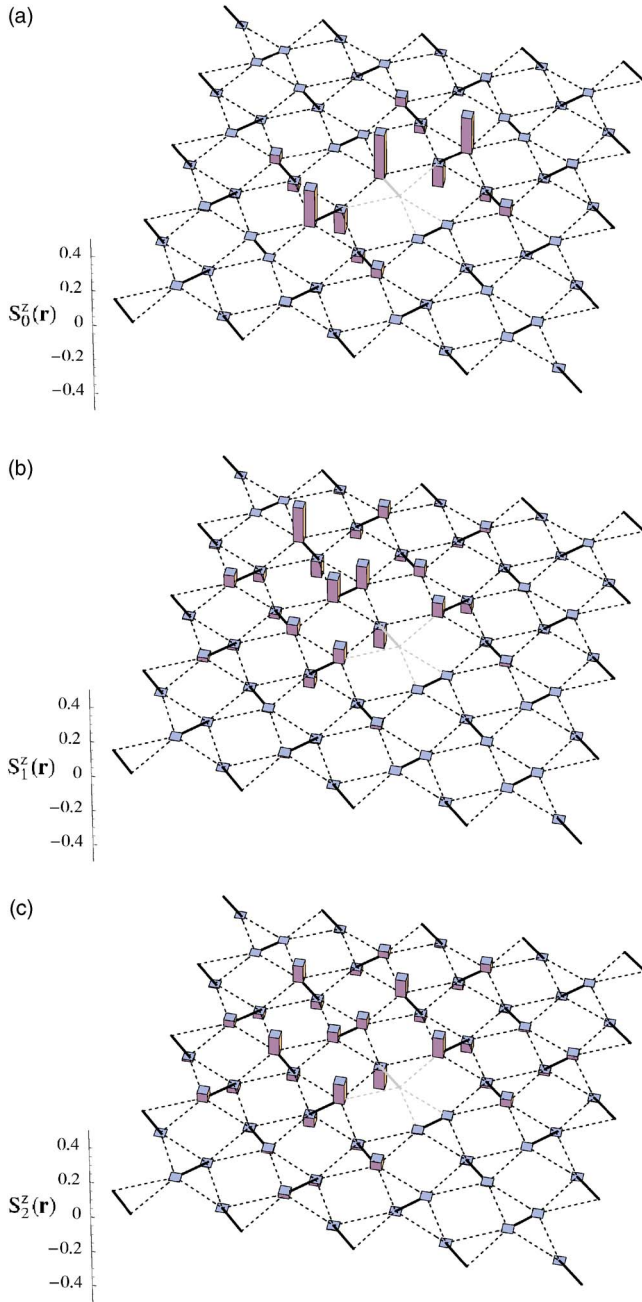


FIG. 3. (Color online) Spin distribution function $S_n^z(\mathbf{r})$ calculated in (a) ground state, (b) first excited state, and (c) second excited state of the 1-hole SS model (1). Calculation was performed for $J=76.8$ K, $J'/J=0.62$, and $M=8$.

In Fig. 3 we also show a spatial distribution of the lowest two excited states of the spin polaron, $S_1^z(\mathbf{r})$ and $S_2^z(\mathbf{r})$, calculated as well in $S^z=1/2$ sector and for $M=8$. In contrast to the $S_0^z(\mathbf{r})$ case, $S_1^z(\mathbf{r})$ shows spin disturbance predominantly along the direction of doped dimer. Intriguingly, this excitation is not centered around the impurity; instead it is shifted away from it towards the neighboring orthogonal dimer. We note, however, that this excited state of the polaron is not confined by the extent of the variational space which allows displacements at much larger distances. This leads to the conclusion that the lowest polaron excitation is centered on

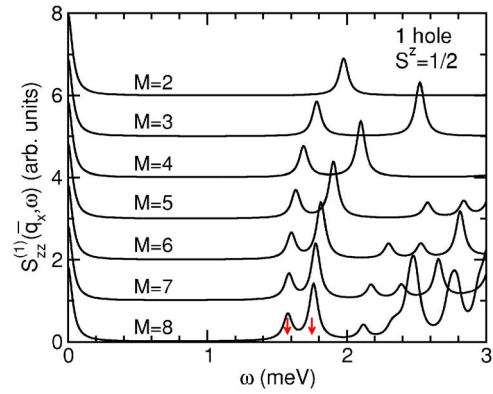


FIG. 4. (Color online) q_x -averaged 1-hole dynamical spin structure factor $S_{zz}^{(1)}(\bar{q}_x, \omega)$ as a function of M calculated for $J=76.8$ K and $J'/J=0.62$. Lines are shifted for clarity. The arrows denote extrapolated positions of the lowest two peaks.

the neighboring orthogonal dimer, yet it remains localized in the vicinity of the hole. A slightly different picture is obtained for $S_2^z(\mathbf{r})$ where the uncompensated spin is distributed more evenly on NN and NNN around the hole. As naively expected, higher energy excitations of the spin polaron spread further away from the impurity site. For this reason more variational states are needed to obtain full convergence in this case.

In the last part we investigate the effect of spin polaron states, forming around static nonmagnetic impurities, on scattering experiments. In Fig. 4 we present the dynamical spin structure factor calculated within our variational approach at finite wave vector \mathbf{q} ,

$$S_{zz}^{(1)}(\mathbf{q}, \omega) = -\text{Im}\langle 0^{(1)} | S_{\mathbf{q}}^z \frac{1}{\omega^+ + E_0^{(1)} - H} S_{-\mathbf{q}}^z | 0^{(1)} \rangle, \quad (4)$$

$$S_{\mathbf{q}}^z = \sum_{\mathbf{R}, \mathbf{r}} e^{i\mathbf{q}(\mathbf{R}+\mathbf{r})} S_{\mathbf{R}, \mathbf{r}}^z.$$

Here \mathbf{R} runs over all unit cells reached within M steps and \mathbf{r} spans four vectors forming the basis of the unit cell that contains two orthogonal dimers. For the details describing interatomic distances in $\text{SrCu}_2(\text{BO}_3)_2$ system we refer the reader to Ref. 18. In addition, a finite $\epsilon=0.25$ meV ($\omega^+=\omega+i\epsilon$) is used to smooth the spectra.

In Fig. 4 we show spectra of $S_{zz}^{(1)}(\bar{q}_x, \omega)$ averaged over the interval of $q_x \in [0, 4]$ (in units of $2\pi/a_0$) for various M . It is evident that spectra at $\omega \lesssim 2$ meV has fully converged, while convergence at higher frequencies is slower. Nevertheless, from Fig. 4 it is apparent that finite doping leads to a finite response of the dynamical spin structure factor at frequencies below the gap value, $\omega \approx 3$ meV, of the undoped system. Similar effect is as well seen in the surface plot presented in Fig. 5 where we explicitly provide the q_x dependence that was computed using 40 discrete values evenly spaced on the interval $q_x \in [0, 4]$. Despite slower convergence at higher frequencies, as observed in Fig. 4, two predictions can be made based on presented calculations. We first predict that in-gap peaks should appear at frequencies far below the gap value in

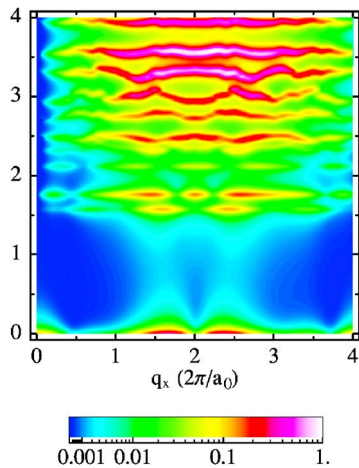


FIG. 5. (Color online) Intensity plot of the 1-hole dynamical spin structure factor $S_{zz}^{(1)}(\mathbf{q}, \omega)$ calculated for $J=76.8$ K, $J'/J=0.62$, and $M=8$. A map was obtained by interpolation between 40 equidistant values of $q_x \in [0, 4]$. Note also the logarithmic intensity scale.

the scattering experiment on a doped $\text{SrCu}_2(\text{BO}_3)_2$ compound, where some Cu atoms would be replaced with static nonmagnetic impurities (holes). These in-gap peaks would carry information about the excited spin-polaron states. Second, doped impurities would contribute to broadening of the one-magnon peak at $\omega \approx 3$ meV through inelastic scattering of magnons on excited states of spin polarons surrounding the impurities. This effect can be clearly seen from Figs. 4 and 5 where extra peaks appear in the vicinity of ω

≈ 3 meV in comparison with calculations on the undoped system.^{15,17}

IV. CONCLUSION

In summary, we presented static and dynamic properties of a single spin polaron in a doped SS lattice. We have developed a variational approach, defined on the infinite lattice, that gives numerically highly accurate results in the thermodynamic limit of static properties of spin polaron and its lowest excitations. The first and second excited state of spin polaron represent $S=1/2$ excitations, their energies lie well within the spin gap of the undoped system. The shape of the spin polaron is highly anisotropic while its extent is well localized in agreement with exact diagonalizations on finite systems.⁸ Spin polaron extends predominantly to the first neighboring dimers lying in perpendicular direction with respect to the dimer containing the impurity. The shape of the first excited state of the polaron extends further in space and is off-centered with respect to the position of the impurity. Spin structure factor of the doped SS model is consistent with the appearance of in-gap peaks and the broadening of the one-magnon peak due to inelastic scattering of the magnon on static spin polarons.

ACKNOWLEDGMENTS

The authors acknowledge the inspiring discussions with B. D. Gaulin that took place during the preparation of this paper. The authors also acknowledge the financial support of Slovene Research Agency under Contract No. P1-0044.

¹P. W. Anderson, *Science* **235**, 1196 (1987).

²R. W. Smith and D. A. Keszler, *J. Solid State Chem.* **93**, 430 (1991).

³H. Kageyama, K. Yoshimura, R. Stern, N. V. Mushnikov, K. Onizuka, M. Kato, K. Kosuge, C. P. Slichter, T. Goto, and Y. Ueda, *Phys. Rev. Lett.* **82**, 3168 (1999).

⁴S. Miyahara and K. Ueda, *J. Phys.: Condens. Matter* **15**, R327 (2003), and references therein.

⁵B. S. Shastry and B. Kumar, *Prog. Theor. Phys. Suppl.* **145**, 1 (2002); B. Kumar and B. S. Shastry, *Phys. Rev. B* **68**, 104508 (2003).

⁶T. Kimura, K. Kuroki, R. Arita, and H. Aoki, *Phys. Rev. B* **69**, 054501 (2004).

⁷C. H. Chung and Y. B. Kim, *Phys. Rev. Lett.* **93**, 207004 (2004).

⁸P. W. Leung and Y. F. Cheng, *Phys. Rev. B* **69**, 180403(R) (2004).

⁹M. Vojta, *Phys. Rev. B* **61**, 11309 (2000).

¹⁰T. Moriya, *Phys. Rev.* **120**, 91 (1960).

¹¹H. Kageyama, M. Nishi, N. Aso, K. Onizuka, T. Yosihama, K. Nukui, K. Kodama, K. Kakurai, and Y. Ueda, *Phys. Rev. Lett.* **84**, 5876 (2000).

¹²B. D. Gaulin, S. H. Lee, S. Haravifard, J. P. Castellan, A. J. Berlinsky, H. A. Dabkowska, Y. Qiu, and J. R. D. Copley, *Phys. Rev. Lett.* **93**, 267202 (2004).

¹³G. A. Jorge, R. Stern, M. Jaime, N. Harrison, J. Bonča, S. E. Shawish, C. D. Batista, H. A. Dabkowska, and B. D. Gaulin, *Phys. Rev. B* **71**, 092403 (2005).

¹⁴S. El Shawish, J. Bonča, C. D. Batista, and I. Sega, *Phys. Rev. B* **71**, 014413 (2005).

¹⁵S. El Shawish, J. Bonča, and I. Sega, *Phys. Rev. B* **72**, 184409 (2005).

¹⁶W. Zheng, J. Oitmaa, and C. J. Hamer, *Phys. Rev. B* **65**, 014408 (2001).

¹⁷C. Knetter, A. Bühler, E. Müller-Hartmann, and G. S. Uhrig, *Phys. Rev. Lett.* **85**, 3958 (2000).

¹⁸C. Knetter and G. S. Uhrig, *Phys. Rev. Lett.* **92**, 027204 (2004).